

How representative are local measurements of the surface shear stress for regional values?

K. Eng ^{*}, W. Brutsaert

Cornell University, 220 Hollister Hall, Ithaca, NY 14853, USA

Received 31 August 2001; received in revised form 23 April 2002; accepted 24 April 2002

Abstract

Local values of surface shear stress measured by eddy correlation devices were compared to regional ones generated by Monin–Obukhov similarity (MOS) theory in the atmospheric surface layer over the cooperative atmosphere–surface exchange study (CASES) area in eastern Kansas. For this comparison, minisodar average wind speed profiles were used to implement MOS. The local surface shear stress values were found to be representative of the regional ones only under free convective conditions. For weak to strongly neutral atmospheric conditions, regional values of the surface shear stress were underpredicted by a factor of two by the locally measured ones. Empirical interpolation equations are proposed to describe the relationship in the intermediate range. The surface roughness values of 0.12 and 0.40 m, respectively, were determined for the two locations of the minisodar sounders by regional analysis of their mean wind speed measurements under neutral atmospheric conditions. The roughness values found in this present study compared well to past investigations conducted in this region. Minisodar roughness values were found in this present study to be a good alternative to radiosonde determined ones.

© 2002 Elsevier Science Ltd. All rights reserved.

Keywords: Land–atmosphere hydrology; Surface shear stress; Neutral atmospheric conditions; Turbulence similarity; Surface roughness; Turbulent surface fluxes

1. Introduction

One way to obtain regional estimates of surface fluxes of momentum, sensible heat, and water vapor makes use of Monin–Obukhov similarity (MOS) theory in the atmospheric surface layer (ASL). In the atmospheric boundary layer (ABL) horizontal length scales tend to be 10–100 times larger than vertical scales, so variables measured at 100 m above the ground are representative for upwind areas with characteristic lengths of 1–10 km. This scale ratio effect allows regional surface fluxes to be calculated from measurements higher up in the boundary layer. By MOS theory, the mean wind speed profile in the ASL can be written as follows [2,11]:

$$\bar{u} = \frac{u_*}{k} \left[\ln \left(\frac{z - d_o}{z_o} \right) - \Psi_{sm}(\zeta) \right], \quad (1)$$

where u_* is the friction velocity (commonly used to represent the surface shear stress, $\tau_o = \rho u_*^2$), k ($= 0.4$) is

von Kármán's constant, z_o is the momentum surface roughness length, \bar{u} is the average (in the turbulence sense) wind velocity at the height z , d_o is the displacement height, $\Psi_{sm}(\cdot)$ is the stability correction function, $\zeta = (z - d_o)/L$ is the dimensionless stability (discussed further in Section 5), and L is the Obukhov length given by

$$L = \frac{-u_*^3}{\frac{kg}{\rho c_p T_a} (H + 0.61 T_a c_p E)}, \quad (2)$$

where H is the specific surface flux of sensible heat, E is the surface evaporation rate, g is the acceleration of gravity, ρ is the density of air, c_p is the specific heat at constant pressure, and T_a is the air temperature near the ground. Measurements of \bar{u} in the ASL and a knowledge of d_o , z_o , and $\Psi_{sm}(\zeta)$ should allow calculation of regional u_* values. These values can be considered as 'regional' (roughly at values from 1 to 10 km) provided the \bar{u} measurements are made at z values which are sufficiently high in the boundary layer (e.g. [3]). Reliable and accurate u_* values are for the purpose of scaling mass and heat transport variables in the ABL.

^{*} Corresponding author.

E-mail addresses: ke21@cornell.edu (K. Eng), whb2@cornell.edu (W. Brutsaert).

In the present study, wind velocity profile measurements obtained with minisodars and surface meteorological observation stations (SMOS) were used to estimate u_* values with (1). These regional estimates of u_* were then compared to locally determined u_* values measured by eddy correlation devices. The objective of this comparison was to determine to what extent these local values of u_* were representative of the regional ones for the area of interest described in Section 4. The effect of atmospheric stability on the relationship between local u_* values and the regional ones was also explored. The minisodar capability to derive z_0 values was tested and compared to values obtained with radiosondes in previous studies [1,8,15] in the same general area.

2. Study area

The present study focused on the cooperative atmosphere–surface exchange study (CASES) site, which encompasses the upper portion of the Walnut Watershed located in Butler County, Kansas [10]. The CASES area may be characterized as flat with the exception of the eastern fringes of this site. The eastern fringes of the area become gradually hilly in the transition toward the Flint Hills to the east. The land is covered predominantly by cropland and some grassland.

3. Instrumentation and data sets

The variables of interest in this study include the hourly wind velocity measurement, \bar{u} , near surface air temperature, T_a , surface sensible heat flux, H , locally measured surface shear stress, u_* , and mixed layer height, z_1 . The \bar{u} values were obtained from two minisodar devices. These devices operate by measuring the intensity and Doppler shift of backscattered acoustic energy from index of refraction fluctuations. These fluctuations are generated typically from temperature and wind fluctuations. T_a values were provided by two SMOS. SMOS stations consist of anemometers for wind measurements, temperature and humidity probes, a barometer, and a rain gauge. H and u_* values were furnished by two eddy correlation devices. The eddy correlation devices are three dimensional sonic anemometers that use wind components and temperature to estimate surface fluxes. The z_1 values were given by the radio acoustic sounding system (RASS). RASS measures in conjunction with the 915 MHz wind profiler (WP). The 915 MHz WP transmits electromagnetic energy into the atmosphere and measures the strength and frequency of the backscattered energy. RASS uses the same operation but sends out sound waves in addition to the electromagnetic energy. The index of refraction

changes by the acoustic wave front are the signal source [6]. A list of all equipment used in this study, location, and measurements provided is given in Table 1.

The data used for the u_* analysis (presented in Section 6) were taken from hourly measurements during the period from 1997 to 1999. The specific dates and times selected for the present study are the same as those listed in [7], Table 4 for unstable atmospheric conditions. The neutral dates and times used for the surface roughness, z_0 , estimation are presented in Tables 2 and 3, and the indicated times on these tables represent the beginning of the hourly periods. The criteria used in the selection

Table 1
Equipment in CASES

Location	Equipment	Measurement	Latitude and longitude
Beaumont, KS	1 Minisodar	Wind profiles (10–200 m)	37 37' 38" 96 32' 19"
	1 SMOS	T_a	
Smileyburg, KS	1 Eddy correlation device	H & u_* (local)	37 31' 15" 96 51' 18"
Whitewater, KS	1 Minisodar	Wind profiles (10–200 m)	37 51' 01" 97 11' 15"
	1 SMOS	T_a	
Towanda, KS	1 Eddy correlation device	H & u_* (local)	37 50' 31" 97 01' 12"

Table 2
List of neutral days and times for 1997

Date	Times (CST)
April 30	1400, 1600
June 28	1300
July 12	0800
July 18	1000
August 14	0800
August 16	0800, 0900, 1900, 2000
August 17	0200
September 16	0900
September 17	0900, 1800

Table 3
List of neutral days and times for 1998

Date	Times (CST)
May 11	1900, 2100, 2300
May 14	0800, 0900, 1700, 1900, 2000
May 17	1800, 1900, 2000
May 18	0900, 1000
May 27	0800
May 29	1000
May 30	0900, 1600, 1700, 1800
May 31	1000
June 5	0400, 0500, 0600, 0700, 0800, 2000
June 14	1700
June 15	0300, 0400
September 26	1400, 1800, 1900, 2000, 2100

of the neutral dates and times will be discussed in detail in Section 4.

4. Estimation of the surface roughness, z_0

The surface parameters z_0 and d_0 must be known in addition to \bar{u} at z (provided by minisodars) and $\Psi(\zeta)$ (discussed in Section 5) in (1) before u_* values can be estimated by means of (1). The simplest way to determine these parameters is from profiles observed under neutral atmospheric conditions, so that $\Psi_{sm}(\zeta)$ goes to zero and (1) reduces to a logarithmic profile. The displacement height, d_0 , was assumed to be negligible, on the basis of earlier findings by [8] for an area in Oklahoma with similar topography as the CASES site; therefore d_0 will be dropped from further consideration in what follows. Wind velocity measurements from balloonborne soundings have been used with (1) under mostly neutral atmospheric conditions to derive u_* and z_0 in a number of previous studies (e.g. [1,5,8,14]), and in one study [12] sodar units were used for this purpose. Serious drawbacks of radiosondes are that they must be disposable, and that their operation tends to be labor intensive. Unlike radiosondes, minisodars are unattended devices which can operate 24 h a day for 365 days of the year to produce wind speeds in the ASL; thus they can provide an abundance of neutral wind profiles for analysis. In this study, 53 minisodar wind profiles, were identified over the time span from 1997 to 1999, which satisfied the imposed criteria for neutrality.

The criteria for neutrality were cloud cover greater than 60%, large wind speed (>10 m/s), the absence of precipitation, and $L \geq \pm 300$ m. This upper limit on L was shown to cause $\Psi_m(\zeta)$ to become negligible in comparison to the $\ln(z/z_0)$ term in (1) [1]. Once $\Psi_m(\zeta)$ can be ignored in (1), determination of u_* and z_0 can be carried out by solving for the slope and intercept of the lower linear portion of the curve on a semilog plot of the equation

$$\bar{u} = b \ln(z) + a, \tag{3}$$

where $b = u_*/k$ and $a = -(u_*/k) \ln z_0$. The adopted procedure to locate the linear portion of the curve on these semilog plots was first to perform a regression by least squares through the three lowest points and a calculation of the coefficient of determination, R^2 . Both calculations were then repeated with these three points and the next highest point. This inclusion of an additional point and recalculation of the regression and R^2 were continued until a maximum value of R^2 was obtained. This procedure was then repeated in reverse starting with three points at the height associated with the maximum value of R^2 by adding successive points downwards towards the three original points. Inspection of the results allowed identification of the set of points

with the highest R^2 value, and thus identified the linear portion where (3) was most applicable. Sample plots are presented as Figs. 1 and 2 to illustrate the identification of the linear region and the application of (3). The average surface roughness values for Beaumont, Kansas and Whitewater, Kansas obtained this way with (3) were 0.40 and 0.12 m, respectively. The individual values for

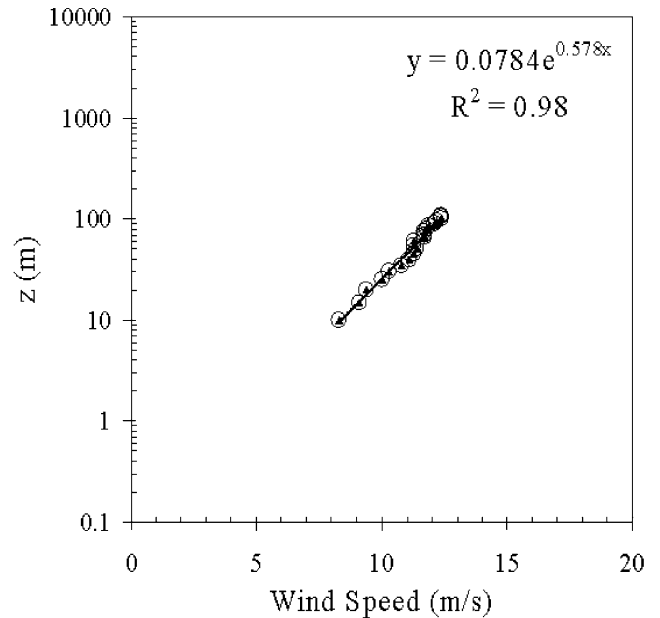


Fig. 1. Example determination of the surface roughness, z_0 , with the Beaumont minisodar on June 14, 1998, 1700 (CST) by means of (3). The resulting values are $z_0 = 0.23$ m and $u_{*L} = 0.69$ m/s.

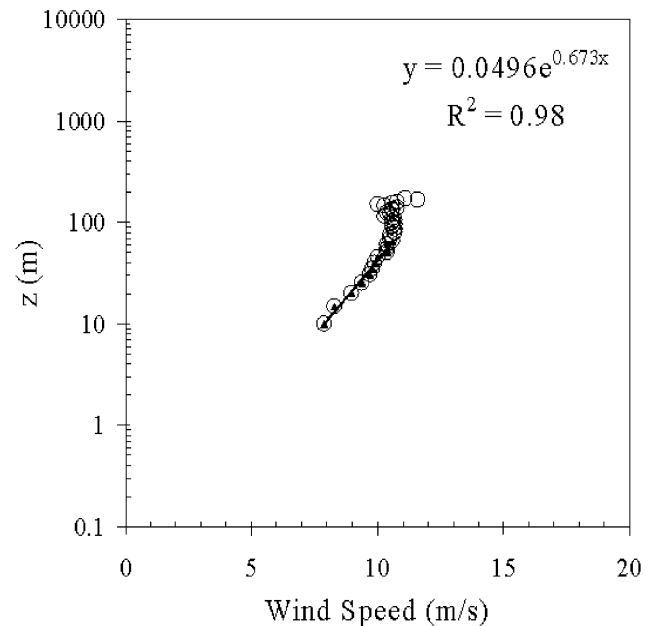


Fig. 2. Same as Fig. 1 but with the Whitewater minisodar on August 16, 1997, 1900 (CST) by means of (3). The resulting values are $z_0 = 0.13$ m and $u_{*L} = 0.59$ m/s.

Table 4
List of neutral days, times, u_{ss} , and z_o for 1997

Date	Times (CST)	Regional		Local	
		u_{ss} (m/s)	z_o (m)	u_{*L} (m/s)	z_o (m)
April 30	1400	1.30	1.00	0.90	0.13
	1600	1.22	1.08	0.79	0.12
June 28	1300	0.85	0.72	0.41	0.01
July 12	0800	0.92	0.60	0.46	0.01
		[0.63]*	[0.11]	[0.35]	[0.004]
July 18	1000	0.73	0.39	0.40	0.01
August 14	0800	0.72	0.23	0.33	0.01
		[0.48]	[0.09]	[0.25]	[0.003]
August 16	0900	1.25	0.81	0.50	0.01
		[0.59]	[0.13]	[0.28]	[0.003]
	1900	0.85	0.51	0.40	0.009
	[0.66]	[0.28]	[0.35]	[0.003]	
	2000	0.66	0.20	0.37	0.009
		[0.65]	[0.29]	[0.32]	[0.003]
	0200	0.71	0.18	0.50	0.01
August 17	0900	0.81	0.28	0.53	0.02
September 16	0900	0.68	0.43	0.55	0.04
September 17	1800	0.77	0.48	0.43	0.01

* [...] indicate measurements taken from the western sampling region.

each of the dates considered are listed in Table 4 for 1997, Tables 5 and 6 for 1998. These values of z_o are consistent with those of earlier studies [1,8,15]. Sugita and Brutsaert [15] found a z_o value of roughly 1 m for the Flint Hills located in eastern Kansas. The Flint Hills are a hillier region to the east of the CASES site. In the study by Jacobs and Brutsaert [8], a z_o value of 0.15 m was determined for a site in Oklahoma west of CASES with similar flat terrain as Whitewater, Kansas in our

Table 5
List of neutral days, part 1, times, u_{ss} , and z_o for 1998

Date	Times (CST)	Regional		Local	
		u_{ss} (m/s)	z_o (m)	u_{*L} (m/s)	z_o (m)
May 11	1900	0.79	0.54	0.38	0.006
	2100	0.87	0.85	0.36	0.007
	2300	0.77	0.50	0.34	0.007
May 14	0800	0.65	0.30	0.40	0.006
	0900	0.70	0.35	0.45	0.006
	1700	0.63	0.13	0.45	0.006
	1900	0.71	0.36	0.385	0.005
	2000	0.85	0.76	0.36	0.005
May 17	1800	1.01	0.85	0.46	0.006
	1900	0.71	0.26	0.42	0.007
	2000	0.88	0.72	0.39	0.008
May 18	0900	0.89	0.60	0.40	0.01
	1000	0.66	0.30	0.36	0.01
May 27	0800	0.66	0.63	0.27	0.01
May 29	1000	0.76	0.26	0.55	0.02
May 30	0900	0.64	0.15	0.43	0.01
	1600	0.65	0.08	0.62	0.01
	1700	0.65	0.08	0.56	0.01
	1800	1.05	0.57	0.53	0.009
May 31	1000	0.86	0.33	0.56	0.02

Table 6
List of neutral days, part 2, times, u_{ss} , and z_o for 1998

Date	Times (CST)	Regional		Local	
		u_{ss} (m/s)	z_o (m)	u_{*L} (m/s)	z_o (m)
June 5	0400	0.72	0.64	0.35	0.03
	0500	0.75	0.55	0.36	0.03
	0600	0.66	0.29	0.40	0.02
	0700	0.63	0.30	0.41	0.02
	0800	0.68	0.37	0.42	0.02
June 14	2000	0.49	0.42	0.30	0.02
	1700	0.69	0.23	0.50	0.04
June 15	0300	0.69	0.61	0.31	0.04
	0400	0.66	0.49	0.29	0.04
September 26	1400	0.83	0.21	0.73	0.03
	1800	0.71	0.32	0.45	0.02
	1900	0.79	0.64	0.35	0.02
	2000	0.85	0.69	0.34	0.02
	2100	0.85	0.72	0.37	0.03
	Avg.	0.78	0.47	0.44	0.02
		[0.58]	[0.16]	[0.29]	[0.003]
	(97–98)	± 0.16	± 0.24	0.13	0.02
		[± 0.09]	[± 0.11]	[0.05]	[0.0005]
	Geomean (97–98)	0.77	0.40	0.43	0.02
	[0.57]	[0.12]	[0.29]	[0.003]	

study. The value of z_o for Beaumont, Kansas in this study is practically identical with the value of $z_o = 0.45$ m obtained in the Washita River basin in Oklahoma by Asanuma et al. [1] for very similar terrain. The u_{*} values generated simultaneously with z_o will be discussed in detail in Section 6.

The local z_o values measured by the three-dimensional sonic anemometers are presented in Tables 4–6 for comparison to the regional ones. The average values of the local z_o for Beaumont, Kansas and Whitewater, Kansas were 0.015 and 0.003 m, respectively. The difference between local and regional values of z_o was due to the scale ratio effect explained in the Introduction. A surface roughness measurement made at a higher elevation in the atmospheric boundary layer will be influenced more by larger obstacles such as tree stands and homes than a measurement made at lower elevations in a micrometeorological station surrounded by grass. Observe, however, that the very small value ($z_o = 0.003$ m) derived for the Whitewater station is based on only six data points; this is hardly representative, so that this value may well be an underestimate.

5. Monin–Obukhov similarity implementation

MOS theory describes the turbulence field in a steady and horizontally homogeneous flow field. This theory states that when turbulence statistics are scaled with the proper variables, they are expressible as universal functions, $\phi()$, of a dimensionless stability parameter, ζ .

The stability correction function, Ψ_{sm} , used in the present study with (1) was proposed in [4] as

$$\Psi_{sm}(y) = \ln(a + y) - 3by^{1/3} + \frac{ba^{1/3}}{2} \ln \left[\frac{(1+x)^2}{(1-x+x^2)} \right] + 3^{1/2}ba^{1/3} \tan^{-1}[(2x-1)/3^{1/2}] + \Psi_o \quad (4)$$

$$\Psi_o = (-\ln a + 3^{1/2}ba^{1/3}\pi/6) \quad (5)$$

where a is 0.33, b is 0.41, y is $-z/L$, and x is $(y/a)^{1/3}$. Eq. (4) is valid for $y \leq b^{-3}$. For $y > b^{-3}$, $\Psi_{sm} = \Psi_{sm}(b^{-3})$ applies. This equation was developed from the three layer model of the ASL proposed on the basis of directional dimensional analysis in [9].

6. Comparison between regional and local u_* estimates

With a known value of the roughness parameter z_o , it is now possible to apply (1) with (4) to determine the surface shear stress u_{*s} (where the subscript s denotes sodar) from the wind profiles under different conditions of atmospheric stability. L was determined by use of near surface air temperatures provided by the SMOS equipment, and surface sensible heat fluxes from the eddy correlation devices. The average wind speed measurements, \bar{u} , from the minisodar were taken over the height range spanning from $50z_o$ to $0.1z_i$ proposed in [3]. Minisodar average wind profiles were discarded that displayed an irregular feature showing a decreasing wind velocity near the top of the ASL, because this is inconsistent with MOS theory. This feature appeared on 37 average wind profiles out of 111 from the minisodars. The values of the mixed layer height, z_i , were determined from analysis of mean virtual potential temperature profiles from radio acoustic sounding systems, and are listed in Table 5 in [7]. Since (1) and (2) both depend on the surface shear stress, an iterative scheme was used to find u_{*s} . The iterative procedure would start with the u_{*L} (where L indicates local) value, and then calculate a new value of u_* which would again be placed into (1). This process would be repeated until the previous and the current calculation of u_* would match. The u_{*s} values could then be compared with those obtained by the local eddy correlation measurements u_{*L} . This was done by plotting the ratios u_{*s}/u_{*L} against the dimensionless stability parameter, $|z_i/L|$, where z_i is the mixed layer height (given in [7], Table 5).

The results showing the dependence of u_* ratio ($= u_{*s}/u_{*L}$) on $|z_i/L|$ obtained by using the wind speed measurements over the ASL height range, are presented in Fig. 3. The linear form of this log–log plot suggests a power law relationship. By linear regression one obtains

$$\frac{u_{*sodar}}{u_{*local}} = 1.94 \left(\left| \frac{z_i}{L} \right| \right)^{-0.105} \quad (6)$$

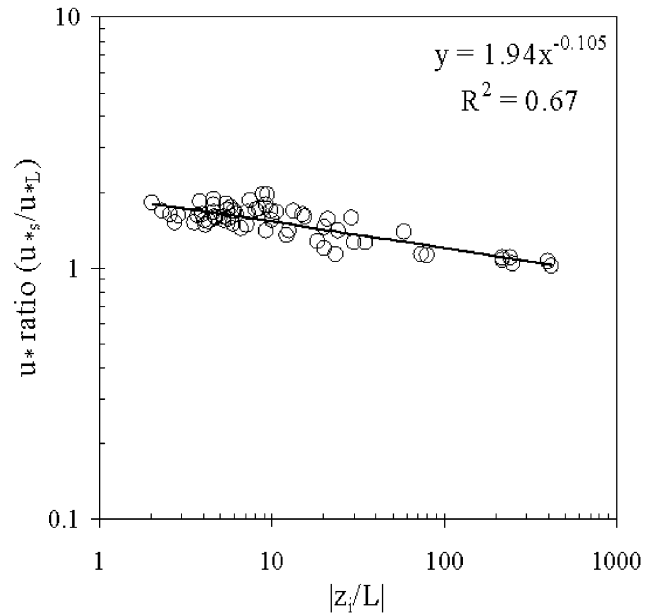


Fig. 3. Relationship between ratio of friction velocities and dimensionless stability for Beaumont and Whitewater, Kansas.

with a coefficient of determination $R^2 = 0.66$. In addition to (6), a second empirical relationship was also tested, namely

$$\left(\frac{u_{*sodar}}{u_{*local}} \right) = \alpha e^{-\beta|z_i/L|} + 1 \quad (7)$$

where α and β are constants. To obtain a ratio of two under neutral conditions α was put at unity and β was found to be 0.04 by visual curve-fitting. This relationship can be seen on Fig. 4. The results shown in Figs. 3 and 4 indicate that under free convective atmospheric conditions (indicated by large $|z_i/L|$ values) u_* values measured locally near the ground are fairly representative of the regional values derived from wind speed measurements higher up in the ASL. These results also indicate that, progressing from free convective to neutral atmospheric conditions, local values of u_* increasingly underpredict the regional ones. Under more neutral atmospheric conditions ($L \geq \pm 300$) the local u_* values underpredict by a factor of around 2. To explore this point further the neutral and near-neutral ratios were replotted separately as shown in Figs. 5 and 6. These figures show that under atmospheric conditions which are close to neutral, the local u_* underpredicted the regional value by a factor close to 2 regardless of the strength of this atmospheric neutrality. The main reason for this difference is undoubtedly the scale ratio effect discussed in the Introduction (see also [3]). Under unstable conditions a few localized thermal plumes are responsible for much of the vertical transport, so that the difference between u_{*L} and u_{*s} is negligible. Under neutral conditions the turbulent transport is more

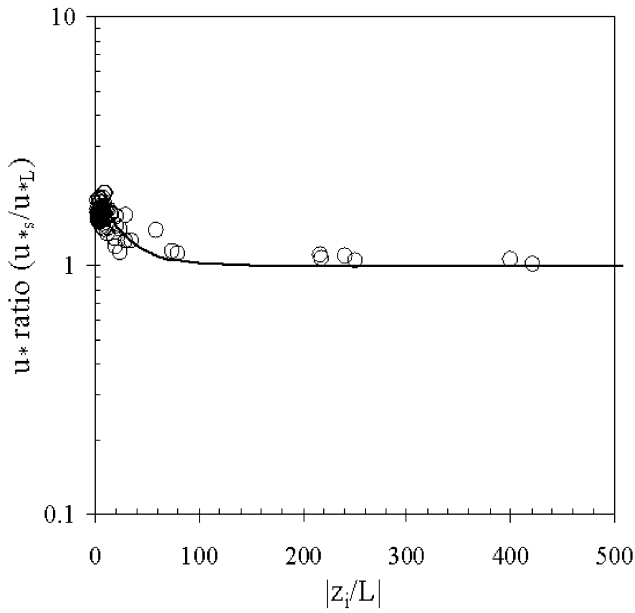


Fig. 4. Second empirical relationship between ratio of friction velocities and dimensionless stability for Beaumont and Whitewater, Kansas.

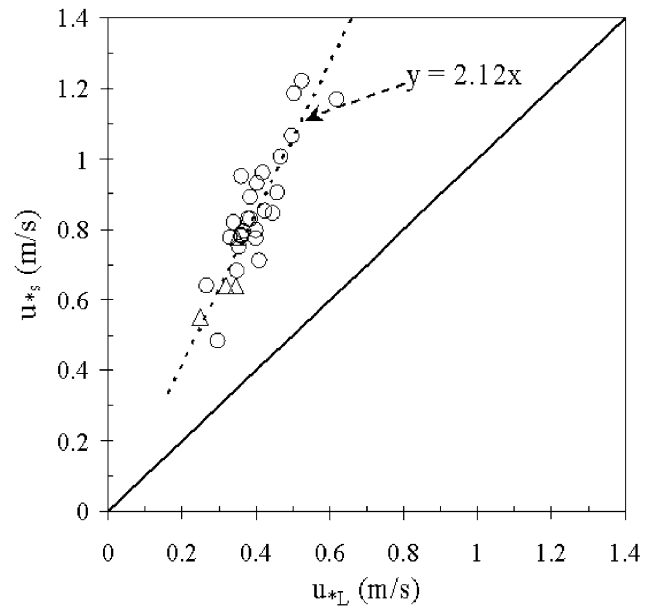


Fig. 6. Local and regional friction velocity comparison for $L \geq \pm 1000$ m for Beaumont/Smileyburg (○) and Whitewater/Towanda (△), Kansas.

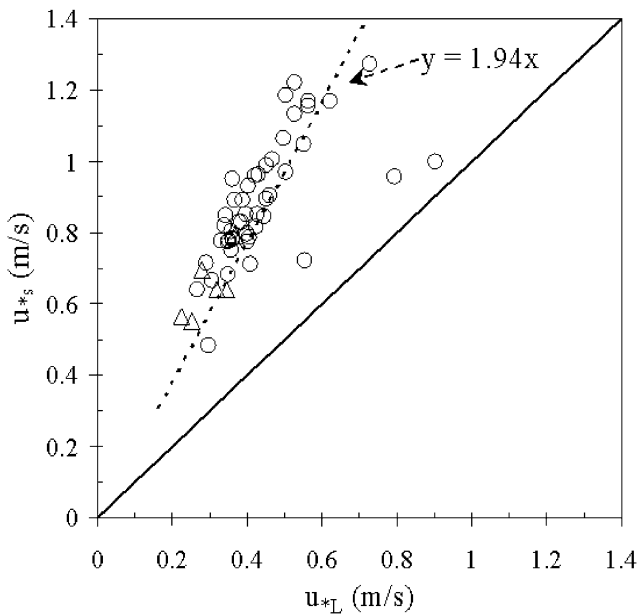


Fig. 5. Local and regional friction velocity comparison for $L \geq \pm 300$ m for Beaumont/Smileyburg (○) and Whitewater/Towanda (△), Kansas.

shear-related, and therefore related to the advective effect of the mean wind; as a result u_{*s} is affected by surface conditions over a larger upwind area. A possible additional reason for this discrepancy between u_{*L} and u_{*s} under near-neutral atmospheric conditions is a ‘turnoff’ effect suggested by Smedman et al. [13]; they attributed this to inactive eddies which may be produced

in the upper portions of the atmospheric boundary layer are then transported down by pressure effects.

7. Conclusions

The present study confirms the applicability of minisodar measurements to estimate surface roughness values (e.g. [12]). The surface roughness values for the CASES experimental area were found to be 0.12 and 0.40 m in the western and eastern portions, respectively. These roughness values are consistent with previous investigations using radiosonde wind measurements in [1,8,15] in the same general area. The inherent strength of continuous and unattended measurements by the minisodar profiler makes it an ideal instrument for this purpose.

The local values of u_* provided by the eddy correlation devices were shown to underestimate the regional ones generated by MOS theory in the ASL to varying degrees. This variability was shown to be dependent on the dimensionless atmospheric stability parameter, $|z_1/L|$. These results indicate that the local u_* values are representative of regional ones under free convective conditions. They also show that local u_* values underpredict the regional ones by a constant factor of around 2, once near-neutral atmospheric conditions are reached. The main reason for this underprediction is probably the turbulence scale ratio effect in the ABL (e.g. [3]). This effect tends to become weaker under convective conditions. A conceivable additional mechanism of this underprediction might be due to a ‘turnoff’

effect by large inactive eddies transported down to the surface; but this will require further study. Two empirical equations of this dependence were tested which should allow prediction of regional u_* from local measurements for similar surface conditions. However extension to other landscapes will probably require further research.

Acknowledgements

This research has been supported, in part, by the National Aeronautics and Space Administration (NAG8-1518) and by the National Science Foundation (ATM-9708622).

References

- [1] Asanuma J, Dias NL, Kustas WP, Brutsaert W. Observations of neutral profiles of wind speed and specific humidity above a gently rolling land surface. *J Meteor Soc Jpn* 2000;78(6):719–30.
- [2] Brutsaert W. *Evaporation into the atmosphere*. Dordrecht, Netherlands: Kluwer Academic Publishers; 1982.
- [3] Brutsaert W. Land-surface water vapor and sensible heat flux: spatial variability, homogeneity, and measurement scales. *Water Resour Res* 1998;34(10):2433–42.
- [4] Brutsaert W. Aspects of bulk atmospheric boundary layer similarity under free-convective conditions. *Rev Geophys* 1999; 37(4):439–51.
- [5] W. Brutsaert and M.B. Parlange, The relative merits of surface layer and bulk similarity formulations for surface shear stress, *J Geophys Res* 1996;101(D23):29, 585–9.
- [6] R. Coulter, Personal communication, 2001 (see also web address gonzalo.er.anl.gov/ABLE/).
- [7] Eng K, Brutsaert W. Vertical velocity variance in the mixed layer from radar wind profilers, submitted for publication.
- [8] Jacobs JM, Brutsaert W. Momentum roughness and view-angle dependent heat roughness at a southern great plains test-site. *J Hydrol* 1998;211:61–8.
- [9] Kader BA, Yaglom AM. Mean fields and fluctuation moments in unstably stratified turbulent boundary layers. *J Fluid Mech* 1990; 212:637–62.
- [10] Lemone MA, Grossman RL, Coulter RL, Wesley ML, Klazura GE, Poulos GS, Blumen W, Lundquist JK, Cuenca RH, Kelly SF, Brandes EA, Oncley SP, McMillen RT, Hicks BB. Land-atmosphere interaction research, early results, and opportunities in the Walnut River watershed in southeast Kansas: CASES and ABLE. *Bull Amer Meteor Soc* 2000;81(4):757–79.
- [11] Monin AS, Yaglom AM. *Statistical fluid mechanics: mechanics of turbulence*, vol. 1. Cambridge, MA: MIT Press; 1971.
- [12] Parlange MB, Brutsaert W. Are radiosonde time scales appropriate to characterize boundary layer wind profiles. *J Appl Meteor* 1990;29(3):249–55.
- [13] Smedman A, Tjernström M, Högström U. The near-neutral marine atmospheric boundary layer with no surface shearing stress: a case study. *J Atmos Sci* 1994;51(23):3399–411.
- [14] Sugita M, Brutsaert W. The stability functions in the bulk similarity formulation for the unstable boundary layer. *Bound-Layer Meteor* 1992;61:65–80.
- [15] Sugita M, Brutsaert W. Wind velocity measurements in the neutral boundary layer above hilly prairie. *J Geophys Res* 1990;95(D6): 7617–24.